

Power Quality Enhancement and Voltage Sag Mitigation by Using an Integrated Nine- Switch Power Conditioner

Sk. Umar , M. Sridhar

Abstract— This paper proposes a novel nine switch converter based integrated power conditioner in place of conventional twelve switch converter based power conditioner for improving power quality. Space vector modulation scheme is proposed for producing gating signals for nine switch converter. In the proposed integrated power conditioner the nine-switch converter replaces shunt and series converters found in conventional back to back power conditioner. Underlying operating principles are discussed comprehensively to demonstrate, how such “series–shunt” replacement can bring forth the full advantages of the nine-switch converter. The shunt and series compensation techniques are discussed and the performance of the proposed nine switch power conditioner is validated through simulations using MATLAB/SIMULINK.

Index Terms— Discontinuous pulse-width modulation, nine switch converter, power conditioner, power quality.

I. INTRODUCTION

POWER quality (PQ) has become an important issue over the past two decades due to the relentless integration of sensitive loads in electrical power systems, the disturbances introduced by nonlinear loads, and the rapid growth of renewable energy sources. Arguably, the most common PQ disturbance in a power system is voltage sags, but other disturbances, such as harmonic voltages and voltage imbalances, may also affect end user and utility equipment leading to production downtime and, in some cases, equipment terminal damage.

Static power converter development has grown rapidly with many converter topologies now readily found in the open literature. Accompanying this development is the equally rapid identification of application areas, where power converters can contribute positively toward raising the overall system quality. In most cases, the identified applications would require the power converters to be connected in series or shunt, depending on the operating scenarios under consideration. In addition, they need to be programmed with voltage, current, and/or power regulation schemes so that they can smoothly compensate for harmonics, reactive power flow, unbalance, and voltage variations. For even more stringent regulation of supply quality, both a shunt and a series converter are added with one of them tasked to perform voltage regulation, while the other performs current regulation. Almost always, these two converters are

connected in a back-to-back configuration, using 12 switches in total and sharing a common dc-link capacitor.

More importantly, a much larger dc-link capacitance and voltage need to be maintained, in order to produce the same ac voltage amplitudes as for the back-to-back converter. Needless to say, the larger dc-link voltage would overstress the semiconductor switches unnecessarily, and might to some extent overshadow the saving of three semiconductor switches made possible by the nine-switch topology. Investigating further by taking a closer view at the existing applications described earlier, a general note observed is that they commonly use the nine-switch converter to replace two shunt converters connected back-to-back. Such replacement will limit the full functionalities of the nine-switch converter. Underlying operating principles are discussed comprehensively to demonstrate how such “series–shunt” replacement can bring forth the full advantages of the nine-switch converter, while yet avoiding those limitations faced by existing applications. Details explaining smooth transitions between normal and sag operating modes are also provided to clarify that the more restricted nine-switch converter will not underperform the more independent back-to-back converter even for sag mitigation.

II. SYSTEM DESCRIPTION AND OPERATING PRINCIPLES OF A NINE-SWITCH POWER CONDITIONER

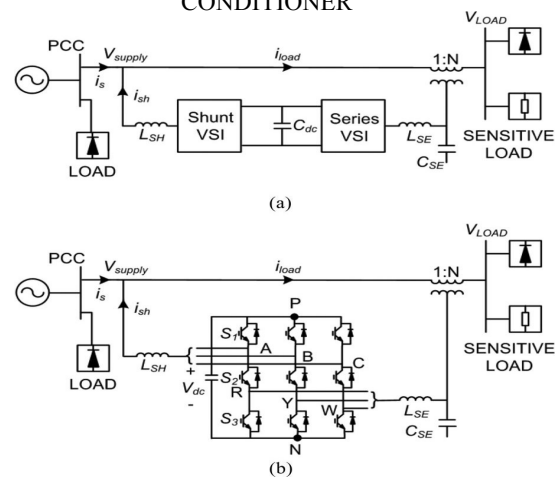


Fig.1. Representations of (a) back-to-back and (b) nine-switch power conditioners.

As illustrated in Fig. 1(b), the nine-switch converter is formed by tying three semiconductor switches per phase, giving a total of nine for all three phases. The nine switches are powered by a common dc link, which can either be a microsource or a capacitor depending on the system requirements under consideration. Like most reduced

component topologies, the nine-switch converter faces limitations imposed on its assumable switching states, unlike the fully decoupled back-to-back converter that uses 12 switches. Those allowable switching states can conveniently be found in Table I, from which, it is clear that the nine-switch converter can only connect its two output terminals per phase to either V_{dc} or 0V, or its upper terminal to the upper dc rail P and lower terminal to the lower dc rail N. The last combination of connecting its upper terminal to N and lower terminal to P is not realizable, hence constituting the first limitation faced by the nine-switch converter. That limitation is nonetheless not practically detrimental, and can be resolved by coordinating the two modulating references per phase, so that the reference for the upper terminal is always placed above that of the lower terminal, as per the two diagrams drawn in Fig. 2. Imposing this basic rule of thumb on reference placement then results in those gating signals drawn in Fig. 2 for the three switches of S₁, S₂, and S₃ per phase. Equations for producing them can also be explicitly stated as

$$S_1 = !S'_1 = \begin{cases} \text{ON,} & \text{if upper reference is larger than carrier} \\ \text{OFF,} & \text{otherwise} \end{cases}$$

$$S_3 = !S'_3 = \begin{cases} \text{ON,} & \text{if lower reference is smaller than carrier} \\ \text{OFF,} & \text{otherwise} \end{cases}$$

$$S_2 = S'_1 \oplus S'_3 \quad (1)$$

where \oplus is the logical XOR operator. Signals obtained from (1), when applied to the nine-switch converter, then lead to those output voltage transitional diagrams drawn in Fig. 2 for representing V_{AN} and V_{RN} per phase. Together, these voltage transitions show that the forbidden state of V_{AN} = 0V and V_{RN} = V_{dc} is effectively blocked off. The blocking is, however, attained at the incurrence of additional constraints limiting the reference amplitudes and phase shift. These limitations are especially prominent for references having sizable amplitudes and/or different frequencies, as exemplified by the illustrative cases shown in Fig. 2(a) and (b). In particular, Fig. 2(a) shows two references of common frequency limited in their phase displacement, while Fig. 2(b) shows two references of different frequencies limited to a maximum modulation ratio of 0.5 each, extendible by 1.15 times if triplen offset is added, in order to avoid crossover. The limited phase-shift constraint, associated with references of the same frequency and combined modulation ratio of greater than 1.15 with triplen offset added (=1.2 in Fig. 2(a) as an example), has recently been shown to adapt well with online uninterruptible power supplies [15], which indeed is a neat and intelligent application of the nine-switch converter. This, however, is only a single application, which by itself is not enough to bring forward the full potential of the nine-switch converter. Considering now the second limitation detailed in Fig. 2(b), a helpful example for explaining it is the nine-switch dual drive system proposed in [13], where references used for modulation can have different operating frequencies. These references are for the two output terminal sets of the nine-switch converter, tied to separate motors operating at approximately the same rated voltage but at different frequencies. Such motor operating criteria would force the references to share the common carrier range equally, like that drawn in Fig. 2(b). The maximum modulation ratio allowed is therefore 0.5 × 1.15 per reference. Even though technically viable, such sharing of carrier is not practically favorable, since to produce the same output voltages, the dc-link voltage maintained, and hence semiconductor stress experienced, must at least be doubled. Doubling of voltage is, however, not needed for the traditional dual converter, whose topological structure is similar to the back-to-back converter, and hence would also support a maximum modulation ratio of unity. Quite clearly then, doubling of dc-link voltage is attributed to the halving of modulation ratios imposed by the nine-switch converter, and is therefore equally experienced by the ac–dc–ac adjustable speed motor drives recommended in [14], where the nine-switch converter is again operating at different frequencies. Judging from these examples, the general impression formed is that the nine-switch converter is not too attractive, since its semiconductor saving advantage is easily shadowed by tradeoffs, especially for cases of different terminal frequencies. Such unattractiveness is however not universal, but noted here to link only with those existing applications reported to date, where the nine-switch converter is used to replace two shunt-connected converters. References

TABLE I
SWITCH STATES AND OUTPUT VOLTAGES PER PHASE

S ₁	S ₂	S ₃	V _{AN}	V _{RN}
ON	ON	OFF	V _{dc}	V _{dc}
ON	OFF	ON	V _{dc}	0
OFF	ON	ON	0	0

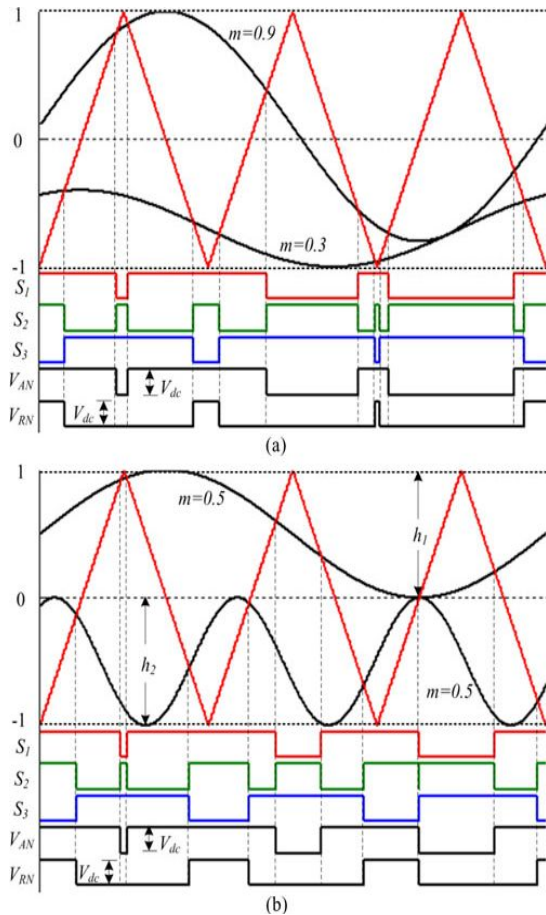


Fig. 2. Arrangements of references having (a) the same frequency but different amplitudes, and (b) different frequencies but the same amplitude.

demanded by these shunt converters are usually both sizable, inferring that the carrier band must be shared equally between them, and hence giving rise to those tradeoffs identified earlier. Therefore, instead of “shunt–shunt” replacement, it is recommended here that the nine-switch converter should more appropriately be used for replacing a series and a shunt converter like those found in a power quality conditioner or any other “series–shunt” topological applications. Explanation for justifying that recommendation is provided in Section II-C with all relevant advantages and residual tradeoffs identified.

Usefull formulas:

$$V^1_\gamma = V_\gamma + V_{SH}, V_{SH} = 1 - \max(V_A, V_B, V_C)$$

$$\gamma = A, B, \text{ or } C$$

$$V^1_\delta = V_\delta + V_{SE}, V_{SE} = -1 - \min(V_R, V_Y, V_W)$$

$$\delta = R, Y, \text{ or } W \quad (2)$$

where $\{M_{SH}, \omega_{SH}, \theta_{SH}\}$ are the modulation ratio, angular frequency, and initial phase of the shunt terminals, and $\{M_{SE}, \omega_{SE}, \theta_{SE}\}$ are the corresponding quantities for the series terminals.

$$H_n(s) = 2K_1\omega_c(s + \omega_c)/(s^2 + 2\omega_c s + \omega_n^2 + \omega_c^2) \quad (3)$$

where K_1 , ω_n , and ω_c represent the gain parameter, chosen harmonic resonant frequency, and cutoff frequency introduced for raising stability, respectively, but at the expense of slight transient sluggishness.

III. EXPERIMENTAL VERIFICATION

To validate its performance, a nine-switch power conditioner was implemented in the laboratory, and controlled using a dSPACE DS1103 controller card.

The dSPACE card was also used for the final acquisition of data from multiple channels simultaneously, while a 4-channel Lecoy digital scopewas simply used for the initial debugging and verification of the dSPACE recorded data, but only four channels at a time. The final hardware setup is shown in Fig. 8, where parametric values used are also indicated.

Other features noted from the figure include the shunt connection of the upper UPQC terminals to the supply side, and the series connection of the lower terminals to the load side through three single-phase transformers. Reversal of terminal connections for the setup, like upper→series and lower→shunt, was also affected, but was observed to produce no significant differences, as anticipated. For flexible testing purposes, the setup was also not directly connected to the grid, but was directed to a programmable ac source, whose purpose was to emulate a controllable grid, where harmonics and sags were conveniently added. With such flexibility built-in, two distorted cases were programmed with the first having a lower total harmonic distortion (THD) of around 4.18%. This first case, being less severe, represents most modern grids, regulated by grid codes, better. The second case with a higher THD of around 11.43% was included mainly to show that the nine-switch UPQC can still function well in a heavily distorted grid, which might not be common in practice. Equipped with these two test cases, experiments were conducted with the shunt compensation scheme. always activated, so as to produce the regulated dc-link voltage needed for overall UPQC operation, on the other hand, was first deactivated, and then activated to produce the two sets of

comparative load voltage data. The data obviously show that the proposed nine-switch UPQC is effective in smoothing the load voltage, regardless of the extent of low order grid harmonic distortion introduced. To strengthen this observation, Fig.4 shows the supply, series injection, and load voltages for the second test case with a higher grid THD, and with both series and shunt compensation activated. The supply voltage is indeed distorted, and would appear across the load if series compensation is deactivated and the transformer is bypassed. The distortion would, however, be largely blocked from propagating to the load, upon activating the series compensation scheme with the shunt compensation scheme still kept executing. Example load voltage waveform illustrating this effectiveness can be found at the bottom of Fig.4. Roughly, the same results were also obtained when the nine switch converter was replaced by its back-to-back

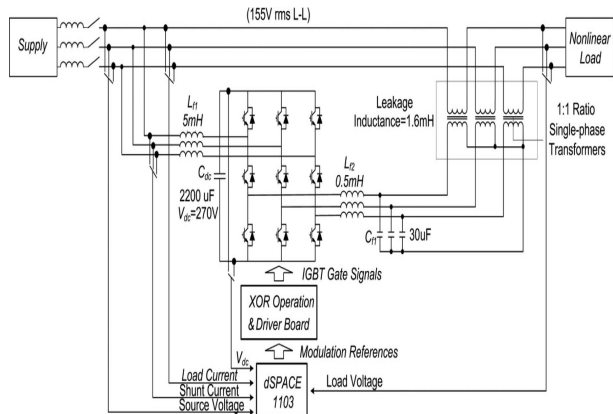


Fig.3. Experimental setup and parameters used for testing.

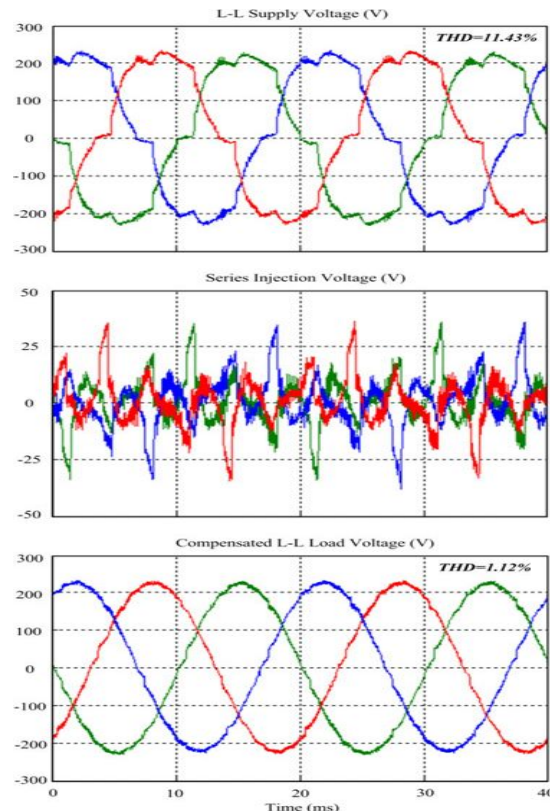
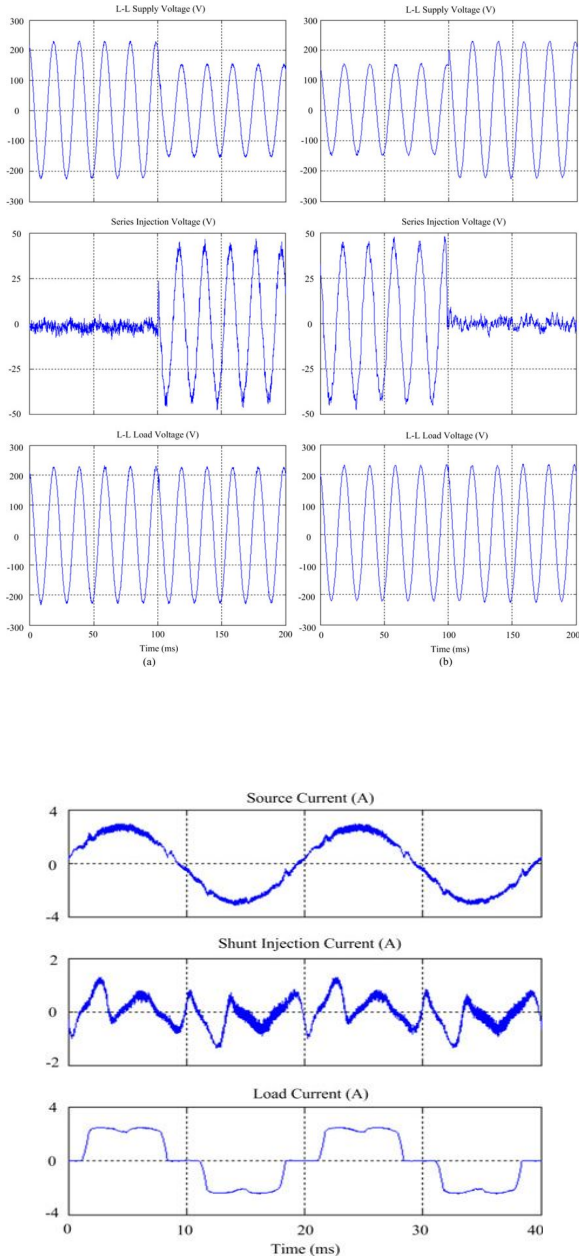


Fig. 4. Experimental supply, series injection, and load voltages captured during normal power conditioning mode.



lesser semiconductor switches, and hence a lower system cost. semi conductor switches, and hence a lower system cost. To next verify its shunt compensating ability, Fig.6 shows the source, shunt injection and load currents conditioned by the nine-switch UPQC. Although the load current is heavily distorted, the shunt control scheme is capable of compensating it, so that the grid current drawn is always sinusoidal, as intended. With the programmable source now configured to introduce a 20% sag, Fig.5 shows the correspondingly sagged grid voltage, series injection voltage, and compensated load voltage during the normal to sag transition and its inverse recovery.

These waveforms collectively prove that the sag has been blocked from propagating to the load, while yet using lesser semiconductor switches. Complementing Fig.5 shows the grid, shunt injection, and load currents during the same normal

to sag transition and its recovery. The grid current is obviously sinusoidal throughout the whole transitional process with an increase in amplitude noted during the period of grid sag. This increase in grid current is transferred to the shunt terminal of the nine switch power conditioner, whose absorbed (negative of injected) current now has a prominent fundamental component, as also reflected by the second row of waveforms plotted in Fig.5.

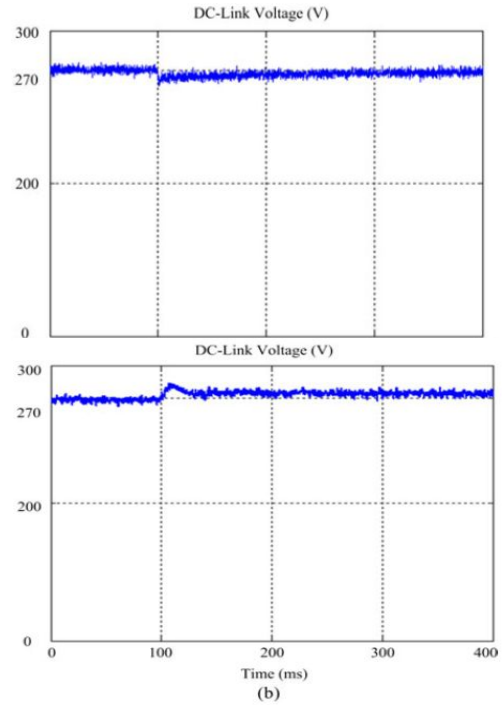


Fig.7. Experimental dc-link voltage during (a) normal-to-sag and (b) sag-to-normal transitions.

Upon processed by the nine-switch power stage, the incremental power associated with the higher shunt current is eventually forced out of the series terminal as an injected voltage, needed for keeping the load voltage and power unchanged. Yet another feature verified through the testing is the dc-link voltage needed by the nine-switch power conditioner, whose value is always higher than that of the back-to-back conditioner, if series compensation is demanded. This increase can, however, be kept small by adopting the carrier division scheme. To confirm that, Fig.7 shows the conditioner dc-link voltage regulated at only 270V throughout the whole sag and recovery process. This dc-link voltage is merely 8% higher than that of the back-to-back case.

CONCLUSION

This paper evaluates shortcomings experienced by previous applications of the newly proposed nine-switch converter. With a better understanding developed, the conclusion drawn is that the nine-switch converter is not an attractive alternative for replacing back-to-back converter with two shunt bridges. Instead, the nine-switch converter is more suitable for replacing back-to-back converter in “series-shunt” systems, where one good example is the UPQC. As a further performance booster, a modified 120°-discontinuous modulation scheme is presented for reducing the overall

commutation count by 33%. Followed up next with proper shunt and series control, harmonics, reactive power, and voltage sags are compensated promptly with no appreciable degradation in performance. The nine-switch conditioner is therefore proved to be effective, while yet using lesser semiconductor switches. Simulation results for confirming its anticipated smooth performance have already been obtained.

REFERENCES

- [1] D. L. Ashcroft, "The static power converter committee—Some perspectives," *IEEE Trans. Ind. Applicat.*, vol. IA-21, no. 5, pp. 1097–1098, Sep. 1985.
- [2] B. Han, B. Bae, H. Kim, and S. Baek, "Combined operation of unified power-quality conditioner with distributed generation," *IEEE Trans. Power Delivery*, vol. 21, no. 1, pp. 330–338, Jan. 2006.
- [3] H. Johal and D. Divan, "Design considerations for series-connected distributed FACTS converters," *IEEE Trans. Ind. Applicat.*, vol. 43, no. 6, pp. 1609–1618, Nov./Dec. 2007.
- [4] T. L. Lee, J. C. Li, and P. T. Cheng, "Discrete frequency tuning active filter for power system harmonics," *IEEE Trans. Power Electron.*, vol. 24, no. 5, pp. 1209–1217, May 2009.
- [5] V. Khadkikar and A. Chandra, "A new control philosophy for a unified power quality conditioner (UPQC) to coordinate load-reactive power demand between shunt and series inverters," *IEEE Trans. Power Del.*, vol. 23, no. 4, pp. 2522–2534, Oct. 2008.
- [6] Y. W. Li, D.M. Vilathgamuwa, and P. C. Loh, "A grid-interfacing power quality compensator for three-phase three-wire microgrid applications," *IEEE Trans. Power Electron.*, vol. 21, no. 4, pp. 1021–1031, Jul. 2006.
- [7] J.W. Kolar, F. Schafmeister, S. D. Round, and H. Ertl, "Novel three-phase ac-ac sparse matrix converters," *IEEE Trans. Power Electron.*, vol. 22, no. 5, pp. 1649–1661, Sep. 2007.
- [8] P. C. Loh, F. Blaabjerg, F. Gao, A. Baby, and D. A. C. Tan, "Pulsewidth modulation of neutral-point-clamped indirect matrix converter," *IEEE Trans. Ind. Applicat.*, vol. 44, no. 6, pp. 1805–1814, Nov./Dec. 2008.
- [9] F. Blaabjerg, S. Freysson, H. H. Hansen, and S. Hansen, "A new optimized space-vector modulation strategy for a component-minimized voltage source inverter," *IEEE Trans. Power Electron.*, vol. 12, no. 4, pp. 704–714, Jul. 1997.
- [10] E. Ledezma, B. McGrath, A. Munoz, and T. A. Lipo, "Dual ac-drive system with a reduced switch count," *IEEE Trans. Ind. Applicat.*, vol. 37, no. 5, pp. 1325–1333, Sep./Oct. 2001.
- [11] M. Jones, S. N. Vukosavic, D. Dujic, E. Levi, and P. Wright, "Five-leg inverter PWM technique for reduced switch count two-motor constant power applications," *IET Proc. Electric Power Applicat.*, vol. 2, no. 5, pp. 275–287, Sep. 2008.
- [12] C. Liu, B. Wu, N. R. Zargari, D. Xu, and J. Wang, "A novel three-phase three-leg ac/ac converter using nine IGBTs," *IEEE Trans. Power Electron.*, vol. 24, no. 5, pp. 1151–1160, May 2009.
- [13] T. Kominami and Y. Fujimoto, "A novel three-phase inverter for independent control of two three-phase loads," in *Proc. IEEE-Ind. Applicat. Soc. (IAS)s*, 2007, pp. 2346–2350.
- [14] T. Kominami and Y. Fujimoto, "Inverter with reduced switching-device count for independent ac motor control," in *Proc. IEEE-IECON*, 2007, pp. 1559–1564.
- [15] C. Liu, B. Wu, N. R. Zargari, and D. Xu, "A novel nine-switch PWM rectifier-inverter topology for three-phase UPS applications," in *Proc. IEEE-Everyday Practical Electron. (EPE)*, 2007, pp. 1–10.
- [16] S. M. Dehghan, M. Mohamadian, and A. Yazdian, "Hybrid electric vehicle based on bidirectional Z-source nine-switch inverter," *IEEE Trans. Veh. Technol.*, vol. 59, no. 6, pp. 2641–2653, Jul. 2010.
- [17] M. J. Newman, D. G. Holmes, J.G. Nielsen, and F. Blaabjerg, "A dynamic voltage restorer (DVR) with selective harmonic compensation at medium voltage level," *IEEE Trans. Ind. Applicat.*, vol. 41, no. 6, pp. 1744–1753, Nov./Dec. 2005.
- [18] M. J. Newman and D. G. Holmes, "A universal custom power conditioner (UCPC) with selective harmonic voltage compensation," in *Proc. IEEEIECON*, 2002, pp. 1261–1266.
- [19] Y. Li, D. M. Vilathgamuwa, and P. C. Loh, "Microgrid power quality enhancement using a three-phase four-wire grid-interfacing compensator," *IEEE Trans. Ind. Applicat.*, vol. 41, no. 6, pp. 1707–1719, Nov./Dec. 2005.
- [20] O. Ojo, "The generalized discontinuous PWM scheme for three-phase voltage source inverters," *IEEE Trans. Ind. Electron.*, vol. 51, no. 6, pp. 1280–1289, Dec. 2004.